TiO_2 Sol-gel Coating as a Transducer Substrate for Impedimetric Immunosensors

R. A. D. de Faria,[a,*] M. Houmard,[b] V. A. M. do Rosário,[c] V. de Freitas Cunha Lins,[a] L. G. D. Heneine,[c] and T. Matencio[d]

[a]Department of Chemical Engineering, Universidade Federal de Minas Gerais, Belo Horizonte, MG 31270-90, Brazil

[b]Department of Materials and Construction Engineering, Universidade Federal de Minas Gerais, Belo Horizonte, MG 31270-90, Brazil

[c]Department of Applied Immunology, Fundação Ezequiel Dias, Belo Horizonte, MG 30510-010, Brazil

[d]Department of Chemistry, Universidade Federal de Minas Gerais, Belo Horizonte, MG 31270-90, Brazil

https://doi.org/10.15255/CABEQ.2019.1699

Original scientific paper
Received: July 4, 2019
Accepted: December 7, 2019

Given the importance of the transducer elements in the performance of sensors for various applications, as well as the growing search for devices that are capable of providing the response in shorter time, in this work, titanium dioxide was examined as a candidate for application in an electrochemical biosensor. A TiO_2 coating deposited by sol-gel method on a silicon wafer was obtained with an anatase crystalline structure, as an n-type semiconductor with donor density equal to $2.954 \cdot 10^{17}$ cm^{-3}. Its surface was functionalized to be tested as a biosensor to detect snake venom of the *Bothrops* genera, and each step of the functionalization was investigated using Electrochemical Impedance Spectroscopy (EIS) and Cyclic voltammetry. Despite being less sensitive than the reference method ELISA, the TiO_2-based biosensor was also capable of detecting the analyte of interest at 20 $\mu g\ mL^{-1}$, revealing an increase in its leakage resistance and phase shift after incubation in this solution. Furthermore, the total time for carrying out the biodetection with the TiO_2-coated device (41.24 ± 0.05 min) was estimated to be approximately 80 % shorter than that required by the labelled standard assay, which indicates that TiO_2 is a promising electrochemical transducer for biosensing applications.

Keywords:
titanium dioxide, biosensor, transducer, Electrochemical Impedance Spectroscopy

Introduction

Firstly described by Clark and Lyons in the 1960s, the term "biosensor" refers to a chemical device that is capable of recognizing an analyte of interest by a biological element, transforming the signal of recognition into a measurable output signal[1].

The considerable growth in the biosensor market is due to its wide range of applications that demand simple, real-time, selective, and non-expensive devices[2] for various applications, such as for food quality monitoring, medical applications, and environmental pollution.

Among the components of a biosensor, the transducer has a crucial role in improving the device's performance[3]. Despite the variety of materials commonly employed as transducers, the electrochemical substrates attract remarkable interest in analytical science especially due to their simplicity, their relatively low cost, and the possibility of their use in portable sensors[4].

A promising candidate for application as an electrochemical transducer in biosensors is titanium dioxide. TiO_2 is an attractive material owing to its high abundance on the planet, low cost, no toxicity, chemical and biological stability, and photocatalytic activity[5]. Nonetheless, it is environmentally friendly and presents a tuneable structure that can vary among anatase, rutile, brookite, and TiO_2 (B)[6]. As a semiconductor, the metal oxide allows the charge transfer phenomena between its surface and the analyte of interest, improving the device's performance[7]. In its various forms (nanotubes, nanosheets, nanoparticles, sol-gel matrices, macropore three-dimensional structure, etc.), TiO_2 has been considered a good material for application as a transducer matrix also due to its morphology and structure that can act as a favourable interface to immobilize different kinds of biological elements of recognition, such as enzymes and antibodies[6]. Despite all these

*Corresponding author: E-mail: ricardo.adriano08@hotmail.com

promising features, most reports have focused on the employment of TiO_2 in photocatalysis processes due to its semiconductor properties, such as in water treatment[8], improvement of air quality[9] and self-cleaning surfaces[10]. In the biosensors field, Bao *et al.*[11] studied the modifications in TiO_2 morphological features to develop a biosensor for glucose measurement by means of protein immobilization. In addition, Liu and Chen[12] reported the employment of a labelled layer of horseradish peroxidase in titania substrates to improve its electro-activity and to provide its capability for biosensing applications. In agreement with the previous authors, Topoglidis *et al.*[13] concluded that the high specific surface area of TiO_2 particles is a key point for the success in biomolecules immobilization, allowing its application as transducer matrix for numerous biological devices.

In this context, the aim of this work was to evaluate the applicability of TiO_2 obtained by the sol-gel method as a transducer matrix for electrochemical biosensors. Herein, the TiO_2 electrode was functionalized with horse antibodies to detect an aqueous solution of snake venom by electrochemical impedance spectroscopy (EIS). In this research, the snakebite diagnosis was chosen to assess the applicability of TiO_2 as an electrochemical substrate in biosensors because of the importance of snake bites in the medicine field.

Once, the only approved treatment method by the World Health Organization (WHO) for combating snake venoms is serotherapy; the accurate identification of the offending snake in an accident is crucial for the administration of the proper antivenom in the victim[14]. The identification of the animal is still challenging, though. In its guidelines for the management of snakebite, the WHO[14] mention that clinicians can recognize the snake if the patient brings it to the hospital after the accident or by means of a description of the animal. However, the institution itself recognizes that both methods are clearly inaccurate and propose some laboratorial methods.

Theakston and Laing[15] cited that the snakebite diagnosis is based on the clinical approach, in which the development of some symptoms are associated with the venom of different snakes, and the performance of laboratorial tests that are complementary in the identification process. In this scenario, many researchers have been devoted to overcome the limitations of the traditional methods for the diagnosis of snakebite. The most commonly employed technique for this purpose is still the enzyme-linked immunosorbent assay (ELISA), which was firstly reported in 1977 by Theakston *et al.*[16] Despite its great accuracy, ELISA possesses some important limitations mainly with respect to the required long time of experimentation[17]. Giri *et al.*[17] point out that other traditional techniques in this context (e.g., radioimmunoassay, agglutination test, and immunofluorescence) are not exclusively very time-consuming, but they also require high cost materials, and sometimes present low sensitivity.

Since the timing of antivenom administration plays a crucial role in the effectiveness of the treatment of the envenomed patients due to the toxicity of the venoms[18], this research also brings special attention to the time response of the proposed TiO_2-based biosensor.

Material and methods

Sol-gel deposition of TiO_2

A precursor sol was prepared according to the methodology described by Houmard *et al.*[19] with absolute ethanol [C_2H_5OH], hydrochloric acid [HCl] and titanium (IV) isopropoxide (TIPT) [$C_2H_{28}O_4Ti$]. The TIPT concentration in the solution was 0.4 M, and the TIPT/H_2O/HCl molar composition used was 1/0.82/0.13. Before use, this solution was aged for 48 h at room temperature.

A commercial (1 0 0) silicon wafer doped n-type was pretreated in piranha solution (H_2SO_4:H_2O_2, 3:1) and in 1 % HF in order to clean this substrate, removing its natural oxide layer[20]. The cleaned wafer was then subjected to a single dip-coating in the sol-gel solution with a 5 mm s^{-1} withdrawal speed. After removal, the as-obtained film was heated in a muffle furnace (Lavoisier 400 D) at 100 °C for 15 minutes to favour the gel development, and to avoid crack formation in the formed film[21]. Finally, the material was heat-treated at 500 °C for 2 h for crystallization.

Characterization of TiO_2 film

Optical microscopy was employed to analyse the TiO_2 coating surface using a BelPhotonics Microscope with a 100x magnification. The structural characterization of the TiO_2 film was carried out by X-ray diffraction (XRD) using a Philips PANalytical PW1710 diffractometer using Cu Kα (λ = 1.540 Å) radiation operating at 40 kV and 40 mA. XRD measurements were taken in a 2θ scan range from 6° to 130°. To avoid the intense signal from the wafer, a grazing incidence XRD was also performed in a θ scan range from 3° to 130° using a step size of 0.06° s^{-1}.

The TiO_2 electro-active area was estimated based on Randles-Sevcik equation[22] by Cyclic Voltammetry (CV) varying the scan rate from 10 to 200 mV s^{-1}. An aqueous solution containing 100 mM of KCl as supporting electrolyte and 1 mM

of $K_3[Fe(CN)_6]$ as redox probe were used to carry out the assay.

Capacitance measurements of the TiO_2 film were carried out by Mott-Schottky analysis by scanning potential from –0.8 to + 1.5 V vs Ag/AgCl (50 mV step height) at 100 Hz as described by Sun *et al.*[23] With this technique, it was possible to estimate the TiO_2 carriers density, as well as identify its n- or p-type doping. The capacitive characteristics of the obtained film provide important information about its electrochemical behaviour and, consequently, its employability as a transducer matrix for electrochemical devices.

Functionalization of the TiO_2 surface

Prior to functionalization, the TiO_2 coating deposited on silicon wafer (1 cm²) was degreased by sonicating in acetone, polysorbate 20 (0.05 % v/v Tween 20), and Millipore Milli-Q water (resistance 18.2 MΩ cm) for 10 minutes. After rinsing the material several times with Milli-Q water, it was immersed in a solution of NH_4OH:H_2O_2:H_2O (ratio of 1:1:7) in dark environment at room temperature for 1 h. Reagent excess was removed by washing the surface with Milli-Q water. The substrate was then incubated in an aqueous solution of 3-aminopropyltriethoxysilane (APTES) 1 %v/v for 1 h, and rinsed with Milli-Q water to remove the excess of silane groups. Subsequently, it was activated with glutaraldehyde 2.5 %v/v for 1 h. After rinsing, the activated TiO_2 silicon slice was incubated in a solution of horse antibodies affinity purified (as described by Heneine and Catty[24]) from the commercial antibothropic serum, produced by Fundação Ezequiel Dias (FUNED, Minas Gerais/Brazil), obtained by the immunization of horses against a venom pool from *Bothrops* snakes. The antibody solution (10 μg mL^{-1}) was prepared in Tris(hydroxymethyl) aminomethane buffer (10 mM Tris buffer, pH 7.4). Another rinsing step was performed to remove unbound antibodies, and the resultant material was finally exposed to a solution of Bovine Serum Albumin (BSA) 1 %w/v for 30 minutes in order to block the active sites of the surface, to inhibit non-specific reactions. The silicon slice containing the self-assembled monolayers was finally rinsed to remove unwanted physically adsorbed molecules. The obtained biosensor was stored in 0.01 M Tris buffer (pH 7.4) at 4 °C until use. All these steps in obtaining the biosensor are presented in Fig. 1.

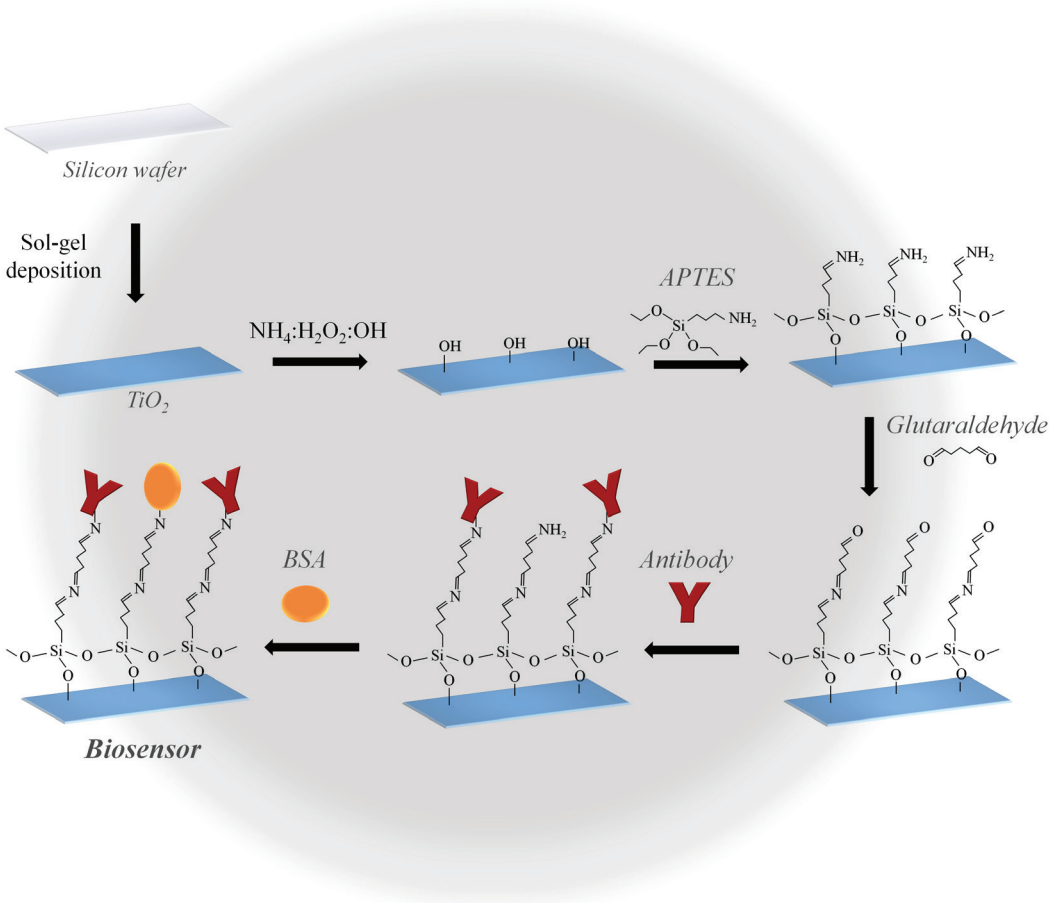

Fig. 1 – *Schematic representation of the steps in obtaining the TiO_2-based biosensor*

Electrochemical monitoring of the functionalization steps

In order to monitor the functionalization procedure, the TiO_2 substrate was subjected to CV and EIS after each step of the biosensor preparation. All the electrochemical measurements were performed in a Princeton Applied Research VersaSTAT 3 potentiostat coupled to a conventional three-electrode cell composed by the TiO_2 surface as working electrode, a platinum counter electrode, and an Ag/AgCl reference electrode.

Impedance spectra were collected in a frequency range from 10^4 to 10^{-2} Hz with potential amplitude of 10 mV at the open circuit potential previously monitored for 300 s. An aqueous 100 mM KCl solution was used as electrolyte.

Ten cycles of CV were carried out at a potential window from –0.4 to +0.8 V vs Ag/AgCl at 50 mV s^{-1} scan rate. An aqueous solution of 100 mM KCl containing 5 mM $K_4[Fe(CN)_6]$ and 5 mM $K_3[Fe(CN)_6]$ was used as electrolyte.

Analyte recognition by the TiO_2 biosensor

EIS was performed in triplicate using the same conditions previously described for the biosensor, before and after its incubation in the analyte solution (20 μg mL^{-1} pool of *Bothrops* venom: *B. jararaca, B. alternatus, B. neuwiedi* and *B. jararacussu*) for 20 minutes. The venoms were provided by FUNED. After this time, the working electrode was exhaustively rinsed with Tris buffer in order to remove the unbound venom molecules from its surface. Impedance data were collected from VersaSTUDIO software, and simulated using Zview software employing the appropriate electrical equivalent circuit.

Analyte recognition by Enzyme-Linked Immunosorbent Assay (ELISA)

ELISA analysis, adapted from the method described by Heneine *et al.*[25], was used as a reference method for detecting snake venom since it is a very useful and sensitive technique for this purpose[26]. Likewise, many authors have described the use of this standard immunoassay to detect the presence of venom in blood or other body fluid samples[24,27,28].

The technique was performed in triplicate by coating overnight at 4 °C a polystyrene 96-well microtitre plate with 100 μL of *Bothrops* snake venom (20 μg mL^{-1} in 0.05 M carbonate buffer, pH 9.6). The wells of the plate were then rinsed with washing solution (0.05 %v/v Tween-20/0.9 %w/v NaCl) in order to remove unbound antigens. A blocking step was carried out by adding 1 %w/v BSA during 1 h at 37 °C. The plate was washed again and then incubated in a 10 μg mL^{-1} solution of horse antibodies produced against bothropic venom diluted in 0.1 M phosphate buffered saline (PBS, pH 8.6). After incubation for 1 h at 37 °C, the plate was washed, and to the wells was added 100 μL per well of anti-horse antibody conjugated to horseradish peroxidase enzyme (SIGMA, diluted at 1:20,000). The plate was incubated as above and the wells washed. A solution containing 1,000 μg mL^{-1} *o*-phenylenediamine and 0.04 %v/v H_2O_2 diluted in 0.1 M citrate buffer pH 4.5 was added (100 μL/well) to the plate. In this step, the colour development was observed for 20 minutes at room temperature, when the reaction was interrupted by adding a 30 %v/v aqueous solution of H_2SO_4. Absorbance at 492 nm was read in a microplate reader (Multiskan GO Microplate Spectrophotometer, Thermo Scientific).

Results and discussion

TiO_2 characterization

Figs. 2(a) and (b) show the optical microscopy images of silicon substrate and TiO_2 film surfaces, respectively. Fig. 2(b) revealed a total coverture on the bare silicon surface (Fig. 2a), exhibiting a homogeneous film of the as-deposited TiO_2. The film was also visible by naked eye owing to the presented blue interference colour, which is typical of a film with thickness of approximately 40 nm and porosity of 25 % according to results obtained by Houmard *et al.*[29] in the same conditions of deposition. Furthermore, as verified by Chen *et al.*[30], the film presented a flat and crack-free surface.

Figs. 3(a) and (b) show the XRD patterns of the TiO_2 coating in the conventional 2θ angle and in the grazing-incidence low θ angle, respectively. The inset shown in Fig. 3(a) indicates a peak at 25° associated with TiO_2 anatase (1 0 1) crystalline phase in agreement with the JCPDS[31] card file number 21-1272 and other literature[32,33]. This peak is not clearly appreciated when analysing the range from 10° to 130° due to the overlapping of a main peak located near 70° corresponding to the silicon crystalline structure of the substrate[34]. However, when carrying out the XRD analysis at low-angle (θ), which is more recommendable for thin film analysis[35], no silicon peak was observed, but only the peak located at about 25° related to the presence of anatase TiO_2, indicating the successful deposition and crystallization of the film through the sol-gel method used in this work.

The Randles-Sevcik equation allowed calculation of the electroactive area of the TiO_2 film, which was equal to 0.0212 cm^2. This value corresponds to only 2.12 % of the geometrical area of the material, confirming its low conductivity. This electrochemi-

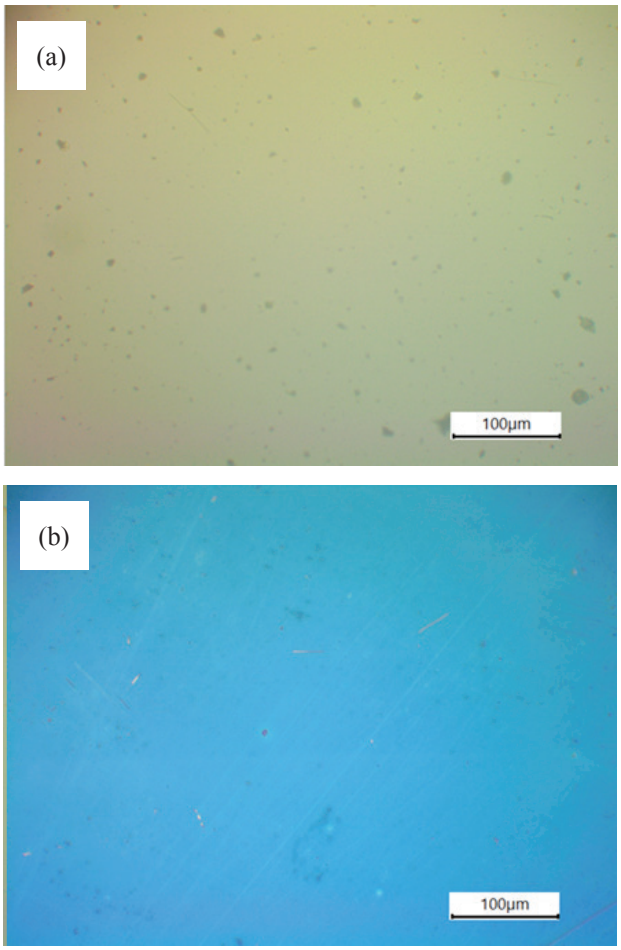

Fig. 2 – *Images of optical microscopy with magnification of 100x of silicon (a) and TiO_2 deposited by sol-gel (b)*

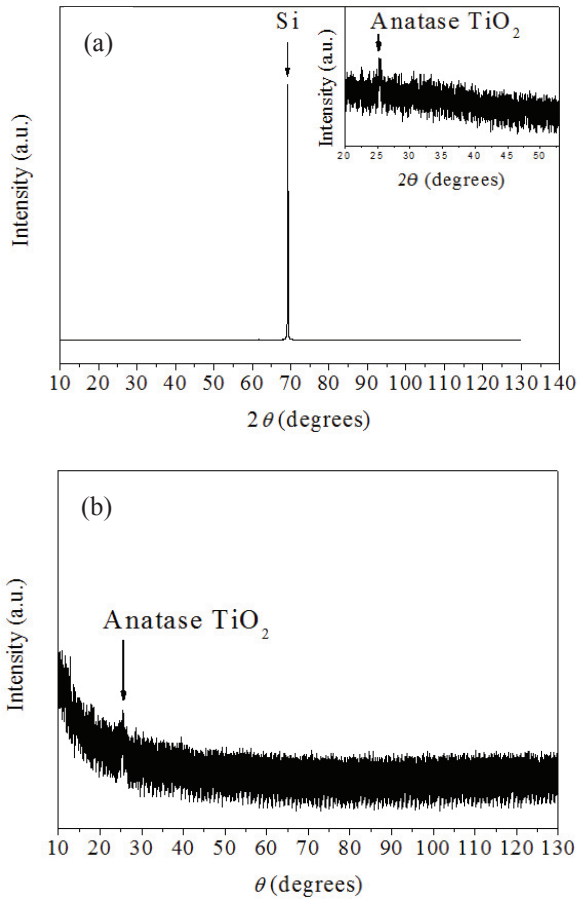

Fig. 3 – *XRD pattern in 2θ scan of the TiO_2 film deposited by sol-gel (the inset is the enlarged view of the diffraction peaks from 20° to 60°) (a) and XRD pattern of the TiO_2 film in grazing-incidence low θ angle (b)*

cal behaviour of TiO_2 anatase was expected due to its large band gap energy (~3.2 eV)[36].

Based on Mott-Schottky equation (eq. 1), which is a widely used technique employed to analyse semiconducting properties of materials[37], the donor density (N_D) of TiO_2 was estimated.

$$\frac{1}{C^2} = \left(\frac{2}{\varepsilon\varepsilon_0 q A^2 N_D}\right)\left(E - E_{fb} - \frac{kT}{q}\right) \qquad (1)$$

where C is the space charge layer capacitance, ε_0 is the permittivity of free space ($8.85 \cdot 10^{-14}$ F cm^{-1})[38], ε is the dielectric constant of TiO_2 equal to 80 according to Sun *et al.*[23], q is the electronic charge ($1.6 \cdot 10^{-19}$ C) that is negative for electrons and positive for holes, A is the geometrical area of the material, E is the applied potential, E_{fb} corresponds to the flat band potential, k is the Boltzmann constant, and T is the absolute temperature.

The Mott-Schottky plot is shown in Fig. 4 and it reveals a linear relationship (R^2 = 0.9957) between the applied potential and C^{-2}. The positive slope indicates that the TiO_2 is an n-type semiconductor as reported in the literature[39].

The N_D of TiO_2, which was obtained from the slope of the Mott-Schottky plot, was equal to $2.954 \cdot 10^{17}$ cm^{-3}, which is consistent with those reported by other authors[23,40]. According to Lamberti *et al.*[39], the electrochemical behaviour of titanium oxides can be related to the presence of defects in its structure, such as oxygen vacancies that can act as donors, improving its carrier concentration and providing more active sites in the semiconductor structure. In order to improve this low carrier density of TiO_2, many research groups have considered doping the semiconductor by introducing defects in its structure, which decreases its band gap value, enhancing the conducting properties of the film[41,42].

Biosensor characterization

Fig. 5(a) shows the monitoring of TiO_2 functionalization steps by CV. Firstly, an increase in both anodic and cathodic peak currents was observed when the substrate was exposed to NH_4OH:H_2O_2:H_2O solution, indicating the incorporation of –OH terminal groups to its surface, since these groups improved the kinetics of electron-transfer phenomenon. After this step, a decrease in elec-

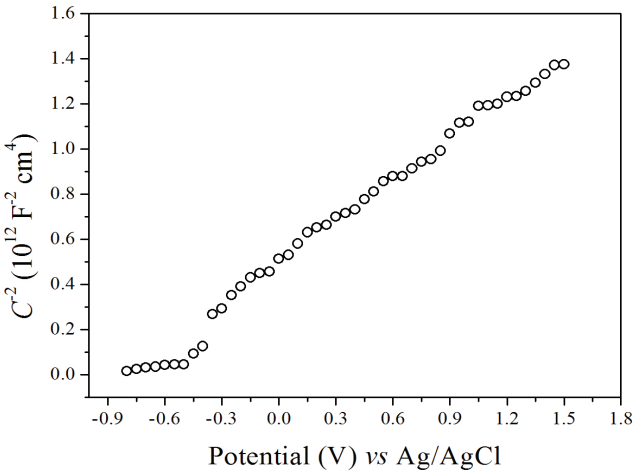

Fig. 4 – *Mott-Schottky plot of TiO_2 in 0.1 M KCl at 100 Hz*

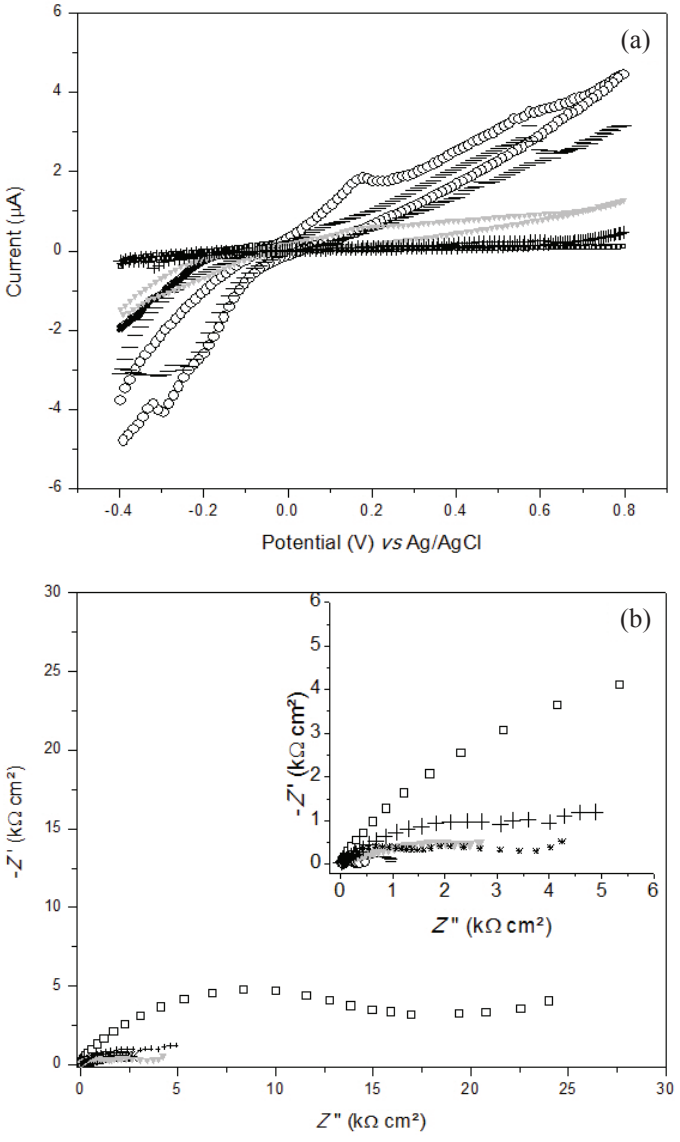

Fig. 5 – *EIS spectrum (a) with inset up to 6 kΩ cm² and cyclic voltammogram (b) of the TiO_2 substrate before (□) and after functionalization with NH_4OH:H_2O_2 (○), APTES (—), glutaraldehyde (*), horse antibodies (▼) and BSA (+)*

trochemical activity of the electrode was observed due to its reaction with APTES. The immobilizing of APTES caused the development of Si-OCH_2CH_3 bonds on the hydroxylated TiO_2, which was confirmed by FTIR by Zhuang *et al.*[43] When glutaraldehyde was attached to the surface, one of the two aldehyde groups of this molecule reacted to the amino group of TiO_2-APTES, leaving the other aldehyde terminal free to bind with the antibody in the next step[44]. Meanwhile, incubating the electrode in horse antibodies solution provoked a new current decrease. The primary amine group of the antibody was supposed to bind the free aldehyde of the electrode, yielding an imine linkage that confers an insulating character to the system and hinders its charge transfer capability[45]. Therefore, a further decrease in current peaks occurred due to the blocking step with BSA, which had an insulator protein structure.

The EIS plot in Fig. 5(b) confirmed the electrochemical behaviour of modified TiO_2 verified by CV. The more insulating the electrode became, the higher was the increase in the semicircle diameter, which is related to the barrier of the charge transfer processes between the electrode surface and the redox probe present in the bulk solution. Thus, the changes in the electrical resistivity of the TiO_2 substrate confirmed the successful development of the biosensor.

Electrochemical biosensor performance

After successful functionalization, the TiO_2-based biosensor was evaluated using EIS technique. EIS is a powerful tool for monitoring electrochemical changes in interfaces, and is often used as a strategy to develop label-free sensors.

Fig. 6(a) and (b) show, respectively, the Nyquist and Bode Diagrams of the device before and after incubation in a 20 μg mL^{-1} solution of the analyte of interest (*Bothrops* venom snake). The Nyquist plots presented a well-defined semicircle owing to resistance and capacitance circuit elements, as well as an almost 45° straight-line in low frequencies, arising to a diffusion limited electrochemical process[46,47]. Despite the fact that Warburg impedance has no physical meaning in non-faradaic sensors (devices whose electrochemical measurements are performed in absence of a redox probe[46]), it has been used in the literature to characterize this kind of sensor[48,49]. The structure of TiO_2 makes it susceptible to the intercalation of small monovalent ions, such as the K^+ from the bulk electrolyte, into the host crystallographic sites generated by the vacancies and interlayers of the matrix[50]. Thus, the Ti^{4+} vacancies are compensated by the counter-ions present in the electrolyte leading to a diffusional barrier to the mass transfer process at low frequencies.

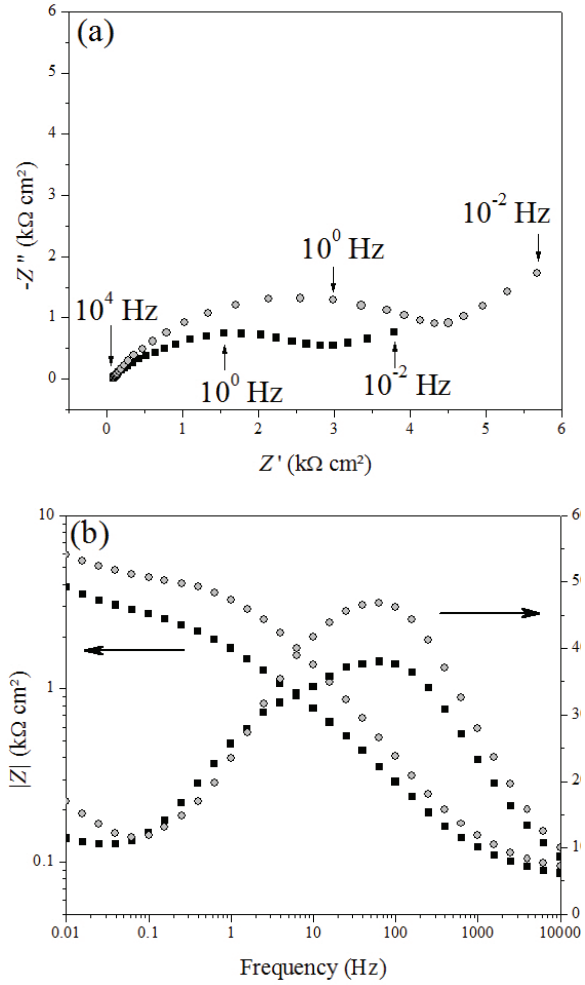

Fig. 6 – *Nyquist plot (a) and Bode plot (b) of magnitude of impedance and phase angle of the TiO_2-based biosensor before (■) and after (●) its exposure to the analyte of interest at 20 μg mL^{-1} in 0.01 M Tris buffer (pH 7.4)*

In order to measure the biosensor response to the analyte of interest, a classical Randles equivalent circuit was employed to fit the impedance data. The employed circuit is shown in Fig. 7, and it was composed by an electrolyte resistance (R_e), a constant phase element (CPE) related to the double layer capacitance, a leakage resistance (R_{leak}), and a Warburg impedance (Z_W), which is associated with the diffusional barrier at low frequencies. The low value of the statistical parameter chi-squared (χ^2 = $6.98 \cdot 10^{-4} \pm 4.64 \cdot 10^{-4}$) ensured the accuracy of the proposed equivalent circuit to model the EIS data in good agreement with the criterion assumed as satisfactory in the literature[51–53].

Accordingly, it was possible to estimate that the increase in the semicircle diameter associated with the exposure to the analyte of interest was associated with an R_{leak} gain of 945.50 ± 350.02 Ω cm². It suggests the formation of the immunocomplex between the antibothropic antibodies present in the

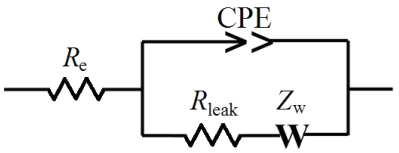

Fig. 7 – *Randles equivalent circuit used to fit impedance data*

electrode surface and the bothropic venom from the bulk solution. The increase in R_{leak} occurs due to the insulating behaviour of both antibody and antigen molecules, which blocks the electronic phenomena on the interface electrode/electrolyte[44,54], in which the impedance is affected by interfacial capacitance or dielectric changes[55]. Similar trend was demonstrated in our previous work[44], in which we fabricated a stainless steel-based immunosensor for the recognition of bothropic venom. Crofer 22 APU (a stainless steel containing approximately 24 % Cr) was used as an impedimetric transducer and the resultant immunosensor exhibited a significant increase in R_{leak} due to the exposure to the venom of *Bothrops* snakes at various concentrations (from 0.1 to 10 μg mL^{-1}). The sensitivity of the Crofer 22 APU-based immunosensor (limit of detection equal to 0.27 μg mL^{-1}) was higher than with the TiO_2-based sensor, possibly due to the higher conductivity of the steel.

The evidence of venom detection was also provided by the notable phase shift and the magnitude impedance increase observed in Fig. 6(b). The phase shift (ϕ) at low frequencies is a consequence of kinetic processes, and is related to the impedance (Z) of the investigated electrochemical system according to eq. 2, in which $|Z|$ is the impedance magnitude, ω corresponds to the radial frequency, and t is time[56].

$$Z = |Z| \frac{\sin(\omega t)}{\sin(\omega t + \phi)} \qquad (2)$$

From the Bode diagram (Fig. 6b), it was possible to estimate that the exposure of the biosensor to the venom solution would generate an increase in the maximum phase angle of 8.82 ± 0.34°, evidencing the successful recognition of the analyte.

In comparison to other sensors reported in the literature, the TiO_2-based biosensor presented major advantages, such as the fact that it is a label-free device, which makes it relatively cheaper, and the short time required for performing the recognition of the snake venom. The total time needed to obtain the impedance result of the EIS assay (including OCP, bare electrode reading, and incubation time) was 41.24 ± 0.05 min. Gao *et al.*[57], for example, developed a sensitive single-bead-based immunofluorescence method for detecting the venom from

Naja kaouthia snakes. Despite the low limit of detection (5 – 10 ng mL^{-1}), the authors performed a more sophisticated functionalization method comprising polystyrene beads and quantum dots as a label and carried out the measurement within 3 h.

Choudhury *et al.*[58] developed a biosensor to detect the venom from Indian cobra by using surface plasmon resonance as a transduction technique and silver film as the optical transducer. In their work, the authors incubated the sensor for a shorter time (12 minutes) in crude cobra venom, but the lowest concentration detectable by their sensor was 100 μg mL^{-1}.

Comparison with ELISA reference method

The impedimetric response of the TiO_2-based biosensor was compared to the reference ELISA technique that is a labelled assay owing to the use of an enzyme conjugate that amplifies the reactivity signals. At the same conditions of analyte concentration and incubation time, the optical immunoassay provided an absorbance at 492 nm of 0.183 for the blank, and 0.999 when it was exposed to the venom solution. This change in optical signal corresponded to an increase of 446.92 ± 4.27 %, whereas the variation of R_{leak} in the impedimetric biosensing was equal to 21.36 ± 14.47 %, and the phase variation shift was equal to 23.36 ± 0.83 %. As also observed by Singh *et al.*[59], the enzyme activity in ELISA makes it superior to many label-free techniques, such as the impedimetric biosensor, thus confirming that it is a difficult challenge to develop a biosensor as sensitive as the labelled-assay. Despite being more sensitive than the impedimetric TiO_2-based biosensor, ELISA presents some disadvantages. It is time-consuming, complex to perform, depends on labelled chemicals that are unstable, compromising the assay robustness, and is more costly[60,61].

In the field of medical diagnosis, the time required to perform the detection tests are one of the major points to be optimized once it can directly impact the efficiency of disease treatments. Mittal *et al.*[62] pointed out the long time required in the diagnosis of breast cancer, and Zhang *et al.*[63] highlighted the time-consuming detection of renal cell carcinoma. Both reports illustrate the trend and importance in developing quick analytical methods for detecting substances of clinical interest.

Despite not being as sensitive as ELISA, the impedimetric TiO_2-based biosensor overcame the time-consuming drawback and the complexity of execution. The analyte detection could be completed within 41.24 ± 0.05 min. On the other hand, according to Paredes *et al.*[64], the traditional ELISA might demand at least 3 hours to be completed.

Conclusion

TiO_2 thin coating was effectively deposited on silicon substrate by sol-gel method. The as-obtained film crystalline structure corresponded to the anatase one with a complete and homogenous coverture. By using Randles-Sevcik equation, the electro active area was found to be smaller than the geometrical one. Mott-Schottky analysis corroborates this low conductivity, indicating that the obtained n-type semiconductor exhibited a relative low donor density. However, the electrochemical impedance spectroscopy and cyclic voltammetry analysis showed that the deposited TiO_2 was successfully functionalized with antibodies against snake venom, and it was capable of detecting this analyte by EIS. When compared to the ELISA reference method under the same venom concentration, the impedimetric biosensor was less sensitive, but it was also less time-consuming. Likewise, other biosensors reported in the literature for detecting different snake venoms consisted of labelled devices with more laborious functionalization steps or presented long time to detect the target analyte. Thus, considering its capability of analyte recognition owing to the changes observed in its electrical behavior by EIS, as well as the required time for analyte detection, it is possible to consider such TiO_2 surface as a promising material for application as an electrochemical transducer in biosensors.

ACKNOWLEDGEMENTS

The authors thank Conselho Nacional de Desenvolvimento Científico e Tecnológico (CNPq), Coordenação de Aperfeiçoamento de Pessoal de Nível Superior (CAPES), Fundação de Amparo à Pesquisa de Minas Gerais (FAPEMIG) for financial support, and Fundação Ezequiel Dias (FUNED) for their technical support.

References

1. International Union of Pure and Applied Chemistry (IUPAC), Electrochemical Biosensors: Recommended definitions and classification. Technical report, Pure Appl. Chem. **71 (**1999) 2333.
2. *Mehrotra, P.,* Biosensors and their applications -A review, J. Oral Biol. Cranio-fac. (2016) 153. doi: https://doi.org/10.1016%2Fj.jobcr.2015.12.002
3. *Manera, M. G., Pellegrini, G., Lupo, P., Bello, V., Fernández, C. J., Casoli, F., Rella, S., Malitesta, C., Albertini, F., Mattei, G., Rella, R.,* Functional magneto-plasmonic biosensors transducers: Modelling and nanoscale analysis, Sens. Actuators B Chem. **239** (2017) 100. doi: https://doi.org/10.1016/j.snb.2016.07.128

4. *Pei, D. N., Gong, L., Zhang, A. Y., Zhang, X., Chen, J.-J., Mu, Y., Yu, H.-Q.,* Defective titanium dioxide single crystals exposed by high-energy {001} facets for efficient oxygen reduction, Nature Commun. **6** (2015) 8696. doi: https://doi.org/10.1038/ncomms9696
5. *Faria, R. A. D., Heneine, L. G. D., Lins, V. F. C., Matencio, T.,* AISI 304 stainless steel as a transducer substrate in electrochemical biosensors for medical applications, Biomed. J. Sci. Technic. Res. **18** (2019) 1. doi: https://doi.org/10.1038/ncomms9696
6. *Yin, Z. F., Wu, L., Yang, H. G., Su, Y. H.,* Recent progress in biomedical applications of titanium dioxide, Phys. Chem. Chem. Phys. **15** (2013) 4844. doi: https://doi.org/10.1039/C3CP43938K
7. *Oliveira, W. F., Arruda, I. R. S., Silva, G. M. M., Machado, G., Coelho, L. C. B. B., Correia, M. T. S.,* Functionalization of titanium dioxide nanotubes with biomolecules for biomedical applications, Mat. Sci. Eng. C **81** (2017) 597. doi: https://doi.org/10.1016/j.msec.2017.08.017
8. *Rojvirron, T., Rojviroon, O., Sirivithayapakorn, S.,* Photocatalytic decolourisation of dyes using TiO_2 thin film photocatalysts, Surf. Eng. **32** (2016). doi: https://doi.org/10.1179/1743294415Y.0000000096
9. *Gauvin, F., Caprai, V., Yu, Q., Brouwers, H. J. H.,* Effect of the morphology and pore structure of porous building materials on photocatalytic oxidation of air pollutants, Appl. Catal. B Environ. **227** (2018) 123. doi: https://doi.org/10.1016/j.apcatb.2018.01.029
10. *Pini, M., González, E. I. C., Neri, P., Siligardi, C. Ferrari, A. M.,* Assessment of environmental performance of TiO_2 nanoparticles coated self-cleaning float glass, Coat. **7** (2017) 8. doi: https://doi.org/10.3390/coatings7010008
11. *Bao, S. J., Li, C. M., Zang, J. F., Cui, X.-Q., Qiao, Y., Guo, J.,* New nanostructured TiO_2 for direct electrochemistry and glucose sensor applications, Adv. Function. Mat. **18** (2018) 591. doi: https://doi.org/10.1002/adfm.200700728
12. *Liu, S., Chen, A.,* Coadsorption of horseradish peroxidase with thionine on TiO_2 nanotubes for biosensing, Langmuir **21** (2005) 8409. doi: https://doi.org/10.1021/la050875x
13. *Topoglidis, E., Campbell, C. J., Cass, A. E. G., Durrant, J. R.,* Factors that affect protein adsorption on nanostructured titania films. A novel spectroelectrochemical application to sensing, Langmuir **17** (2001) 7899. doi: https://doi.org/10.1021/la010309b
14. World Health Organization (WHO), Expert Committee on Biological Standardization: sixtyeighth report. Geneva: WHO Tech. Rep. Series, **1011** (2018).
15. *Theakston, E. D. G., Laing, G. D.,* Diagnosis of snakebite and the importance of immunological tests in venom research, Toxins **6** (2014) 1667. doi: https://doi.org/10.3390/toxins6051667
16. *Theakston, R. D., Lloyd-Jones, M. J., Reid, H. A.,* Microelisa for detecting and assaying snake venom and venom-antibody, Lancet **2** (1977) 639. doi: https://doi.org/10.1016/S0140-6736(77)92502-8
17. *Giri, A., Jagli, D., Panada, N. S. A., Gawde, V.,* Venom detector: A smart approach to detect snake venom, Int. J. Comp. Sci. Inf. Tech. **5** (2014) 35. doi: https://doi.org/10.1.1.639.6568
18. *Sanhajariya, S., Duffull, S. B., Isbister, G. K.,* Pharmacokinetics of snake venom, Toxins **10** (2018) 1. doi: https://doi.org/10.3390/toxins10020073
19. *Houmard, M., Vasconcelos, D. C. L., Vasconcelos, W. L., Berthomé, G., Joud, J. C., Langlet, M.,* Water and oil wettability of hybrid organic-inorganic titanate-silicate thin films deposited via a sol-gel route, Surf. Sci. **603** (2009) 2698. doi: https://doi.org/10.1016/j.susc.2009.07.005
20. *Kumar, A., Mondal, S., Kumar, S. G., Rao, K. S. R. K.,* High performance sol-gel spin-coated titanium dioxide dielectric based MOS structures, Mat. Sci. Semicond. Process. **40** (2015) 77. doi: https://doi.org/10.1016/j.mssp.2015.06.073
21. *Aun, D. P., Houmard, M., Mermoux, M., Latu-Romain, L., Joud, J. C., Berthomé, G., Buono, V. T. L.,* Development of a flexible nanocomposite TiO_2 film as a protective coating for bioapplications of superelastic NiTi alloys, Appl. Surf. Sci. **375** (2016) 42. doi: https://doi.org/10.1016/j.apsusc.2016.03.064
22. *Aghazada, S., Ren, Y., Wang, P., Nazeeruddin, M. K.,* Effect of donor groups on the performance of cyclometalated ruthenium sensitizers in dye-sensitized solar cells, Inorg. Chem. **56** (2017) 13437. doi: https://doi.org/10.1021/acs.inorgchem.7b02164
23. *Sun, M., Zhang, X., Li, J., Cui, X., Sun, D., Lin, Y.,* Thermal formation of silicon-doped TiO_2 thin films with enhanced visible light photoelectrochemical response, Electrochem. Commun. **16** (2012) 26. doi: https://doi.org/10.1016/j.elecom.2011.12.015
24. *Heneine, L. G. D., Catty, D.,* Species-specific detection of venom antigens from snakes of the *Bothrops* and *Lachesis* genera, Toxicon. **31** (1993) 591. doi: https://doi.org/10.1016/0041-0101(93)90114-X
25. *Heneine, L. G. D., Santos, M. R. A., Carvalho, A. J. D., Gontijo, S. S.,* A capture Enzyme-Linked Immunosorbent Assay for species-specific detection of *Bothrops* venoms, J. Immunoass. **20** (1999) 91. doi: https://doi.org/10.1080/01971529909349316
26. *Theakston, R. D. G., Laing, G. D.,* Diagnosis of snakebite and the importance of immunological tests in venom research, Toxins **6** (2014) 1667. doi: https://doi.org/10.3390/toxins6051667
27. *Lee, C. H., Lee, Y. C., Liang, M. H., Leu, S. J., Lin, L. T., Chiang, J. R., Yang, Y. Y.,* Antibodies against venom of the snake *Deinagkistrodon acutus*, Appl. Environ. Microbiol. **82** (2016) 71. doi: https://doi.org/10.1128/AEM.02608-15
28. *Shaikh, I. K., Dixit, P. P., Pawade, B. S., Waykar, I. G.,* Development of dot-ELISA for the detection of venoms of major Indian venomous snakes, Toxicon. **139** (2017) 66. doi: https://doi.org/10.1016/j.toxicon.2017.10.007
29. *Houmard, M., Riassetto, D., Rouseel, F., Bourgeois, A., Berthomé, G., Joud, J. C., Langlet, M.,* Enhanced persistence of natural super-hydrophilicity in TiO_2-SiO_2 composite thin films deposited via a sol-gel route, Surf. Sci. **602** (2008) 3364. doi: https://doi.org/10.1016/j.susc.2008.09.016
30. *Chen, W., Kirihara, S., Miyamoto, Y.,* Fabrication of three-dimensional micro photonic crystals of resin incorporating TiO_2 particles and their terahertz wave properties, J. Am. Ceram. Soc. **90** (2007) 92. doi: https://doi.org/10.1111/j.1551-2916.2006.01377.x
31. Joint Committee on Powder Diffraction Standards (JCPDS), Card No. 21–1272 Powder Diffraction File (1969) Swarthmore, PA.
32. *Su, D., Dou, S., Wang, G.*, Anatase TiO_2: Better anode material than amorphous and rutile phases of TiO_2 for Na-ion batteries, Chem. Mat. **27** (2016) 6022. doi: https://doi.org/10.1021/acs.chemmater.5b02348

33. *El-Deen, S. S., Hashem, A. M., Ghany, E. A., Indris, S., Ehrenberg, H., Mauger, A., Julien, C. M.,* Anatase TiO_2 nanoparticles for lithium-ion batteries, Ionics (2018) 1. doi: https://doi.org/10.1007/s11581-017-2425-y
34. *Pethuraja, G. G., Welser, R. E., Sood, A. K., Lee, C., Alexander, N. J., Efstathiadis, H., Haldar, P., Harvey, J. L.,* Effect of Ge incorporation on bandgap and photosensitivity of amorphous SiGe thin films, Mat. Sci. Appl. **3** (2012) 67. doi: https://doi.org/10.4236/msa.2012.32010
35. *Lee, B., Park, I., Yoon, J., Park, S., Kim, J., Kim, K. W., Chang, T., Ree, M.,* Structural analysis of block copolymer thin films with grazing incidence small-angle X-ray scattering, Macromol. **38** (2005) 4311. doi: https://doi.org/10.1021/ma047562d
36. *López, R., Gómez, R.,* Band-gap energy estimation from diffuse reflectance measurements on sol–gel and commercial TiO_2: A comparative study, J. Sol-Gel Sci. Tech. **61** (2012) 1. doi: https://doi.org/10.1007/s10971-011-2582-9
37. *Liu, J., Yang, H., Tan, W., Zhou, X., Lin, Y.,* Photovoltaic performance improvement of dye-sensitized solar cells based on tantalum-doped TiO_2 thin films, Electrochim. Acta. **56** (2010) 396. doi: https://doi.org/10.1016/j.electacta.2010.08.063
38. *Pu, P., Cachet, H., Sutter, E. M. M.,* Electrochemical impedance spectroscopy to study photo-induced effects on self-organized TiO_2 nanotube arrays, Electrochim. Acta **55** (2010) 5938. doi: https://doi.org/10.1016/j.electacta.2010.05.048
39. *Lamberti, A., Garino, N., Sacco, A., Bianco, S., Chiodoni, A., Gerbaldi, C.,* As-grown vertically aligned amorphous TiO_2 nanotube arrays as high-rate Li-based micro-battery anodes with improved long-term performance, Electrochim. Acta **151** (2015) 222. doi: https://doi.org/10.1016/j.electacta.2014.10.150
40. *Wolcott, A., Smith, W. A., Kuykendall, T. R., Zhao, Y., Zhang, J. Z.,* Photoelectrochemical water splitting using dense and aligned TiO_2 nanorod arrays, Small **5** (2009) 104. doi: https://doi.org/10.1002/smll.200800902
41. *Munir, S., Shah, S., Hussain, H., Khan, R. A.,* Effect of carrier concentration on the optical band gap of TiO_2 nanoparticles, Mat. Des. **92** (2016) 64. doi: https://doi.org/10.1016/j.matdes.2015.12.022
42. *Alim, M. A., Bak, T., Atanacio, A., Plessis, J. D., Zhou, M., Davis, J., Nowotny, J.,* Electrical conductivity and defect disorder of tantalum-doped TiO_2, J. Am. Ceram. Soc. **100** (2017) 4088. doi: https://doi.org/10.1111/jace.14959
43. *Zhuang, W., Zhang, Y., Zhu, J., An, R., Li, B., Mu, L., Ying, H., Wu, J., Zhou, J., Chen, Y., Lu, X.,* Influences of geometrical topography and surface chemistry on the stable immobilization of adenosine deaminase on mesoporous TiO_2, Chem. Eng. Sci. **193** (2016) 142. doi: https://doi.org/10.1016/j.ces.2015.09.005
44. *Faria, R. A. D., Lins, V. F. C., Nappi, G. U., Matencio, T., Heneine, L. G. D.,* Development of an impedimetric immunosensor for specific detection of snake venom, BioNanoSci. **8** (2018) 1. doi: https://doi.org/10.1007/s12668-018-0559-7
45. *Canbaz, M. Ç., Sezgintürk, M. K.,* Fabrication of a highly sensitive disposable immunosensor based on indium tin oxide substrates for cancer biomarker detection, Anal. Biochem. **446** (2014) 9. doi: https://doi.org/10.1016/j.ab.2013.10.014
46. *Daniels, J. S., Pourmand, N.,* Label-free impedance biosensors: Opportunities and challenges, Electroanal. **19** (2007) 1239. doi: https://doi.org/10.1002/elan.200603855
47. *Qu, J., Lou, T., Kang, S., Du, X.,* Laccase biosensor based on graphene-chitosan composite film for determination of hydroquinone, Anal. Lett. **47** (2014) 1564. doi: https://doi.org/10.1080/00032719.2013.867499
48. *Kamakoti, V., Selvam, A. P., Shanmugam, N. R., Muthukumar, S., Prasad, S.,* Flexible molybdenum electrodes towards designing affinity based protein biosensors, Biosens. **6** (2016). doi: https://doi.org/10.3390/bios6030036
49. *Solis-Marcano, N. E., Lopes-Nieves, M., Pinto-Pacheco, B., Cabrera, C. R.,* Capacitive biosensing technique for the detection of DNA modification and hybridization process using custom made gold interdigital microelectrode arrays. In: 46th International Conference on environmental Systems (2016) Vienna, Austria.
50. *Reeves, K. G., Ma, J., Fukunishi, M., Salanne, M., Komaba, S., Dambournet, D.,* Insights into L^+, Na^+, and K^+ intercalation in lepidocrocite-type layered TiO_2 structures, ACS Appl. Energy Mat. **1** (2018) 2078. doi: https://doi.org/10.1021/acsaem.8b00170
51. *Fan, L., Tang, F., Reis, S. T., Chen, G., Koenigstein, M. L.,* Corrosion resistances of steel pipes internally coated with enamel, Corr. **73** (2017) 1335. doi: https://doi.org/10.5006/2497
52. *Garcia-Cabezon, C., Martin-Pedrosa, F., Blanco-Val, Y., Rodriguez-Mendez, M. L.,* Corrosion properties of a low-nickel austenitic porous stainless steel in simulated body fluids, Corr. **74** (2018) 683. doi: https://doi.org/10.5006/2720
53. *Faria, R. A. D., Iden, H., Heneine, L. G. D., Matencio, T., Messaddeq, Y.,* Non-enzymatic impedimetric sensor based on 3-aminophenylboronic acid functionalized screen-printed carbon electrode for highly sensitive glucose detection, Sens. **19** (2019) 1686. doi: https://doi.org/10.3390/s19071686
54. *Zhu, D., Li, Q., Pang, X., Liu, Y., Wang, X., Chen, G.,* A sensitive electrochemical impedance immunosensor for determination of malachite green and leucomalachite green in the aqueous environment, Anal. Bioanal. Chem. **408** (2016) 5593. doi: https://doi.org/10.1007/s00216-016-9660-3
55. *Xu, Q., Davis, J. J.,* The diagnostic utility of electrochemical impedance, Electroanal. **26** (2014) 1. doi: https://doi.org/10.1002/elan.201400035
56. *Bonanni, A., Loo, A. H., Pumera, M.,* Graphene for impedimetric biosensing, Trends in Anal. Chem. **37** (2012) 37. doi: https://doi.org/10.1016/j.trac.2012.02.011
57. *Gao, R., Zhang, Y., Gopalakrishnakone, P.,* Single-bead-based immunofluorescence assay for snake venom detection, Biotech. Prog. **24** (2008) 245. doi: https://doi.org/10.1021/bp070099e
58. *Choudhury, S. N., Konwar, B., Kaur, S., Doley, R., Mondal, B.,* Study on snake venom protein-antibody interaction by surface plasmon resonance spectroscopy, Photonic Sens. **8** (2018) 193. doi: https://doi.org/10.1007/s13320-018-0501-1
59. *Singh, K. V., Bhura, D. K., Nandamuri, G., Whited, A. M., Evans, D., King, J., Solanki, R.,* Nanoparticle-enhanced sensitivity of a nanogap-interdigitated electrode array impedimetric biosensor, Langmuir **27** (2011) 13931. doi: https://doi.org/10.1021/la202546a

60. *Tokarzewicz, A., Romanowicz, L., Sveklo, I., Matuszczak, R., Hermanowicz, A., Gorodkiewicz, E.,* SPRI biosensors for quantitative determination of matrix metalloproteinase-2, Anal. Met. **9** (2017) 2407.
doi: https://doi.org/10.1039 / C7AY00786H

61. *He, Q., Lei, H., Luo, S., Tang, P., Peng, X., Wang, X.,* Liquid crystal biosensor for detecting ischemia modified albumin, Res. Chem. Interm. **43** (2017) 353.
doi: https://doi.org/10.1007/s11164-016-2626-4

62. *Mittal, S., Kaur, H., Gautam, N., Mantha, A. K.,* Biosensors for breast cancer diagnosis: A review of bioreceptors, biotransducers and signal amplification strategies, Bios. Bioelectron. **88** (2017) 217.
doi: https://doi.org/10.1016/j.bios.2016.08.028

63. *Zhang, L., Yu, C., Gao, R., Niu, Y., Li, Y., Chen, J., He, J.,* An impedimetric biosensor for the diagnosis of renal cell carcinoma based on the interaction between 3-aminophenyl boronic acid and sialic acid, Bios. Bioelectron. **92** (2017) 434.
doi: https://doi.org/10.1016/j.bios.2016.10.083

64. *Paredes, J. C. M., Oliveira, L. G., Braga, A. C., Trevisol, I. M., Roehe, P. M.,* Development and standardization of an indirect ELISA for the serological diagnosis of classical swine fever, Pesq. Vet. Bras. **29** (1999) 3.
doi: http://doi.org/10.1590/S0100-736X1999000300006